# Experimental Observation of Anisotropic Magnetic Turbulence in a Reversed Field Pinch Plasma

Y. Ren, A. F. Almagri, G. Fiksel, S. C. Prager, J. S. Sarff, and P. W. Terry

*Center for Magnetic Self-Organization in Laboratory and Astrophysical Plasmas, Department of Physics, University of Wisconsin-Madison, Madison, Wisconsin, USA*

(Received 6 May 2011; published 31 October 2011)

In this Letter we report an experimental study of fully developed anisotropic magnetic turbulence in a laboratory plasma. The turbulence has broad (narrow) spectral power in the perpendicular (parallel) direction to the local mean magnetic field extending beyond the ion cyclotron frequency. Its $k_\perp$ spectrum is asymmetric in the ion and electron diamagnetic directions. The wave number scaling for the short wavelength fluctuations shows exponential falloff indicative of dissipation. A standing wave structure is found for the turbulence in the minor radial direction of the toroidal plasma.

DOI: 10.1103/PhysRevLett.107.195002 PACS numbers: 52.35.Ra, 52.35.Bj, 52.55.Hc

Magnetic turbulence occurs in many plasma settings, including astrophysical plasmas and laboratory experiments [1–3]. This turbulence is fundamental to processes such as the conversion of plasma flow into magnetic energy, conversion of magnetic energy to thermal energy, and the transport of particles, energy, and momentum [4–6]. It is often associated with magnetic reconnection processes. Significant effort has been devoted to understanding the turbulent cascade of magnetic energy and its features, such as its anisotropy and scaling behavior [1,7–9]. Dissipation processes operating within the turbulent cascade are less studied, especially kinetic dissipation that is likely essential to heating and particle energization. Measurements in the solar wind have been a primary driver for research on magnetic turbulence [7]. However, it is now clear that magnetic turbulence in laboratory plasmas shares important features with its astrophysical counterpart, including an MHD inertial range, anisotropy, kinetic dissipation, particle heating and energization, and spectral conversion to ion scale motions. Experiments are therefore an essential counterpart to astrophysical observations to improve the understanding of the magnetic turbulent cascade and its consequences to important processes. Experiments can also circumvent some challenges, such as interpreting frequency spectra to infer the fundamental wave number spectra, which are directly measurable in the laboratory.

In this Letter, we report measurements of fully developed magnetic turbulence in a laboratory plasma, resolved from the driving scale to the ion gyroradius scale. The plasma is a reversed field pinch (RFP), unstable to tearing modes that drive a turbulent cascade with clear scaling characteristics. The turbulent fluctuation energy is anisotropic relative to the large-scale confining magnetic field, concentrated in a narrow range of $k_\parallel$ and a much broader range of $k_\perp$. This anisotropy persists for frequencies characteristic of MHD turbulence to beyond the ion cyclotron frequency. The $k_\perp$ spectrum is also asymmetric with respect to the direction the fluctuations propagate. The wave number scaling for the short wavelength fluctuations shows exponential falloff indicative of dissipation. The spectrum fits well a functional form that is the product of a power-law and exponential falloff, which agrees with recent modeling for dissipation-range turbulence [9], a more fundamental approach than a multiple power-law fit. The inferred scale for onset of strong dissipation is larger than expected for classical dissipation, implying kinetic processes are important. This could be related to powerful noncollisional ion heating reported for RFP plasmas [10–12]. Lastly, we show that the small-scale turbulence has a standing wave radial structure, an important clue as to the type of fluctuation, which has not yet been identified. These comprehensive measurements provide improved insight on the nature of the magnetic turbulence cascade and its connections to processes like particle heating and energization.

The experiments are carried out on the MST RFP [13], with major radius 1.5 m and minor radius 0.5 m. Magnetic probes with multiple pickup coils (10 turns, 1 mm in length and 3 mm in diameter) are inserted into the edge of low current 200 kA deuterium plasmas to measure the equilibrium and fluctuating magnetic field. The line-average electron density is $n \approx 10^{19}$ m$^{-3}$, and the central electron temperature $T_e(0) \approx 180$ eV. The magnetic probe has two sets of four coils which simultaneously measure $B_P$ (poloidal component) and $B_T$ (toroidal component). For each set, one coil measures the local equilibrium magnetic field (using analog integrators), and the other three coils are used for fluctuation measurements. To maximize the dynamic range, the $\dot{B}$ signals are sampled at 10 MHz with an instrumental bandwidth of 2.5 MHz. The two-dimensional spectral density of the magnetic fluctuations, $S(k_P, k_T, f)$, is obtained by extending the two-point correlation method [14] to two dimensions. Pickup coils separated in the poloidal or toroidal direction determine the poloidal or toroidal wave numbers, $k_P$ and $k_T$, respectively. These wave numbers are resolved for all frequencies, $f$, within the instrumental bandwidth. The spatial separation of the coils is $\sim$0.5 cm, allowing a measured wave number

 

bandwidth $-2\pi < k < 2\pi$ cm$^{-1}$, but the data are found to be statistically significant only for $|k| \lesssim 1.5$ cm$^{-1}$. A second probe with a linear array of 7 coils uniformly separated by 1 cm is used to obtain the radial correlation of the fluctuations. Both probes were calibrated to have an absolute error of 5 G for equilibrium measurements and a relative uncertainty less than 10% for $\dot{B}$ signals.

The MST plasma exhibits a quasiperiodic sawtooth relaxation cycle during which the tearing-mode-driven magnetic reconnection bursts and the fluctuation level increases [15]. The insert in Fig. 1 shows a typical fluctuation $\tilde{B}_T$ at $r/a = 0.96$ (from measured $\dot{B}_T$) during a sawteeth cycle with larger magnetic fluctuations at $t = 0$, corresponding to the "crash" time. Conditional averaging of many sawtooth events allows the cycle dynamics to be temporally resolved [10,16]. Figure 1 shows ensemble-averaged power spectra of $\tilde{B}_T$ at two time periods, "between crash" and "during crash" (see the shaded regions in the insert). The peaks around 20 kHz correspond to the unstable core-resonant tearing modes which dominate the spectrum. Their finite frequency results primarily from plasma rotation. Therefore 5–20 kHz is labeled the "tearing mode range". These tearing modes have been studied extensively in RFP research [17]. At higher frequencies the spectra show no distinct features indicative of separate instability and remain smooth beyond the ion cyclotron frequency range ($\sim$ 600 kHz in the edge region) out to 2 MHz, highly suggestive that nonlinear coupling drives a turbulent energy cascade originating from the unstable tearing modes. This is further supported by the factor of 10 or so increase in $\tilde{B}_T$ at nearly all frequencies during the crash when the tearing mode amplitudes burst higher. For reference in discussion, the band 50–200 kHz is labeled the "Alfvén range" since Alfvén waves would appear with these frequencies, and the band $\sim$400–800 kHz is labeled the "ion cyclotron range."

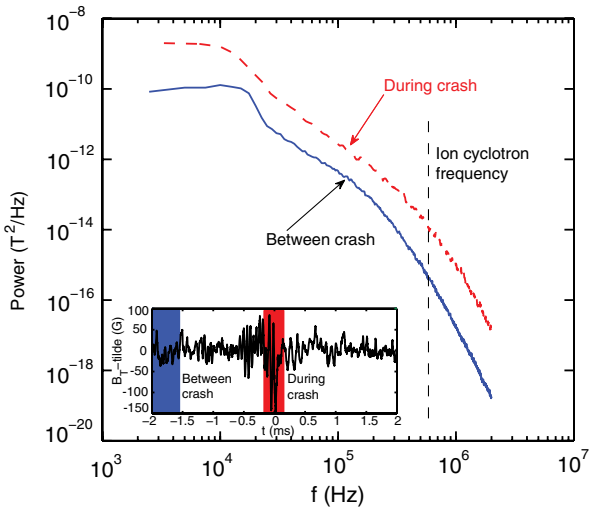


FIG. 1 (color online). The power spectra of $\tilde{B}_T$ between (solid line) and during (dashed line) the sawtooth crash with a typical $\tilde{B}_T$ at $r/a = 0.96$ for the sawtooth cycle as an insert. The vertical line denotes the ion cyclotron frequency ($\approx$ 600 kHz). The shaded region on the left of the inserted plot denotes "between crash," and the shaded region in the middle denotes "during crash."

The anisotropy of the magnetic turbulence can be seen in Fig. 2, where the green arrows indicate the mean (equilibrium) magnetic field direction, and the thick black lines denote the direction perpendicular to the equilibrium field. The upper panels show the spectral density function $S(k_P, k_T, f)$ integrated over the three characteristic frequency ranges: (a) 5–20 kHz (tearing mode range), (b) 50–200 kHz (Alfvén range), (c) 400–800 kHz (ion cyclotron range) for "during crash" measurements. The fluctuations in the tearing mode range do not exhibit strong anisotropy because they are global modes whose resonant surfaces in the core of plasma are far from the probe measurements. On the other hand, $S(k_P, k_T)$ in both the Alfvén range and ion cyclotron range is spread along the direction perpendicular to the local equilibrium field, with $\Delta k_\perp \gg \Delta k_\parallel$, where $\Delta k_\perp$ and $\Delta k_\parallel$ are the spectral width perpendicular and parallel to the local equilibrium magnetic field, respectively. Note that the equilibrium field in the region of probe measurements is dominantly poloidal, $B_P \gg B_T$.

The magnetic probe was scanned radially to measure the radial profiles of the equilibrium and fluctuating magnetic

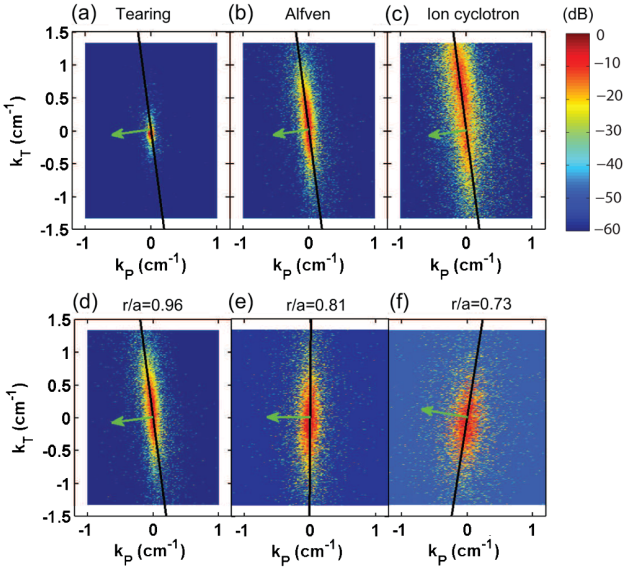


FIG. 2 (color online). The spectral density function $S(k_P, k_T)$ "during crash" in three frequency ranges: (a) tearing, (b) Alfvén, and (c) ion cyclotron, and at three radial locations (for the Alfvén range): (d) $r/a = 0.96$, (e) $r/a = 0.81$, and (f) $r/a = 0.73$. The green arrows denote the direction of the equilibrium magnetic field and the thick black lines show the field-perpendicular direction. The fluctuation power is normalized to its peak value in each plot, and the colors denote normalized fluctuation power in $dB$.

field. The equilibrium field is strongly sheared in the RFP, including a radius where $B_T = 0$ (the reversal surface). The lower panels of Fig. 2 show $S(k_P, k_T)$ for the Alfvén range at three radii spanning the reversal surface: (d) $r/a = 0.96$, (e) 0.81, (f) 0.73, all obtained "during crash." The $S(k_P, k_T)$ spectrum maintains local anisotropy as the equilibrium magnetic field changes direction. The radial correlation length for the turbulence in the Alfvén range (and ion cyclotron range) must therefore be significantly less that the radial separation (7.8 cm) of these measurements, confirmed more directly by correlation measurements discussed below. Although not shown here, the anisotropy in the turbulence is qualitatively the same for "between crash" measurements.

We summarize that an anisotropy in the turbulence power spectrum parallel and perpendicular to the mean field is present for frequencies higher than the tearing mode range, and at all radial positions. The magnetic turbulence has a preference to spread its energy perpendicular to the equilibrium magnetic field, and the spread in magnetic energy along the equilibrium field is much narrower. This observed anisotropy is consistent with MHD turbulence theories and numerical simulations [18–20], but since the anisotropy is observed even beyond ion cyclotron frequency range, it is a more general feature than predicted by MHD. Furthermore, we would like to point out that there exists a physics explanation for the anisotropy of MHD turbulence: a background magnetic field suppresses fast variations along a strong background field since it takes more energy to stretch and bend field lines than to translate them [18].

The spectrum-wide increase in fluctuation power at the sawtooth crash as seen in Fig. 1 is very suggestive that the high frequency fluctuations result from a nonlinear cascade driven by the unstable tearing modes. This is best evaluated through the scaling of the wave number power spectra, obtainable in MST without invoking the Taylor hypothesis [21]. The local $S(k_\parallel)$ and $S(k_\perp)$ spectra are obtained from the measured 2D spectrum $S(k_P, k_T) = \int S(k_P, k_T, f)df$ using $k_\parallel = (k_P B_P + k_T B_T)/B$ and $k_\perp = (k_T B_P - k_P B_T)/B$, where $B = \sqrt{B_P^2 + B_T^2}$. Then $S(k_\parallel) = \int S(k_\parallel, k_\perp)dk_\perp$ and $S(k_\perp) = \int S(k_\parallel, k_\perp)dk_\parallel$. The $S(k_\perp)$ spectra corresponding to the "between crash" and "during crash" cases are shown in Fig. 3. A third case is also shown for separate experiments in which the tearing instability is *reduced* using inductive current profile control, called pulsed parallel current drive (PPCD) [22]. Between these three cases, the fluctuation power in the tearing modes (shaded region $k_\perp \approx 0.05$ cm$^{-1}$) spans a factor of 100, and the power in the shorter wavelength turbulence rises and falls in concert with the tearing modes. Not shown here, the anisotropy in the higher frequency magnetic turbulence described above also appears in PPCD plasmas.

The wave number fluctuation spectra exhibit both power-law and exponential scaling behavior. To illustrate

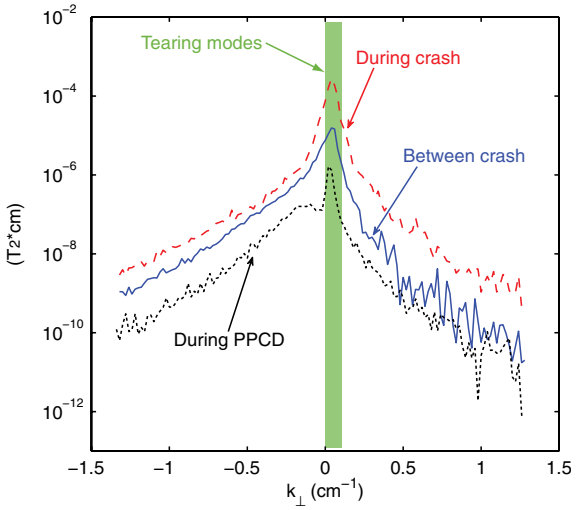


FIG. 3 (color online). The $k_\perp$ spectra for "between crash" (solid line), "during crash" (dashed line), and "during PPCD" (dotted line). The shaded region denotes wave numbers corresponding to tearing modes.

this, the spectra measured at $r/a = 0.96$ "during crash" are plotted in Fig. 4 on a log-log scale for $k > 0$ and a semilog scale for $k < 0$. It can be seen that the fluctuation power has much wider spread in the $S(k_\perp)$ spectrum than in the $S(k_\parallel)$ spectrum; the $S(k_\parallel)$ spectrum is symmetric in $k_\parallel$, and is well described by a broadband power law with steep falloff, $S(k_\parallel) \sim |k_\parallel|^{-5.4\pm0.5}$. On the other hand, the $S(k_\perp)$ spectrum is asymmetric with respect to the direction the fluctuations propagate. This is not a Doppler effect attributable to equilibrium plasma flow. We are not aware of any existing turbulence theory that predicts such behavior. While $S(k_\perp)$ exhibits a power-law character, $S(k_\perp) \sim |k_\perp|^{-4\pm0.2}$, in the ion diamagnetic drift direction ($k_\perp > 0$),

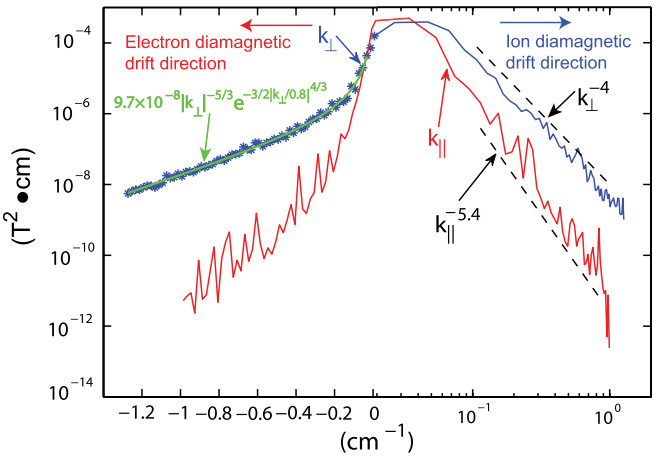


FIG. 4 (color online). The $k_\perp$ (blue solid line and asterisks) and $k_\parallel$ (red solid line) spectra and their scaling characteristics at $r/a = 0.96$ with fittings using power laws (black dashed lines) and using a dissipation-range spectrum (green solid line). The drift direction is meaningful only for the $k_\perp$ spectrum.

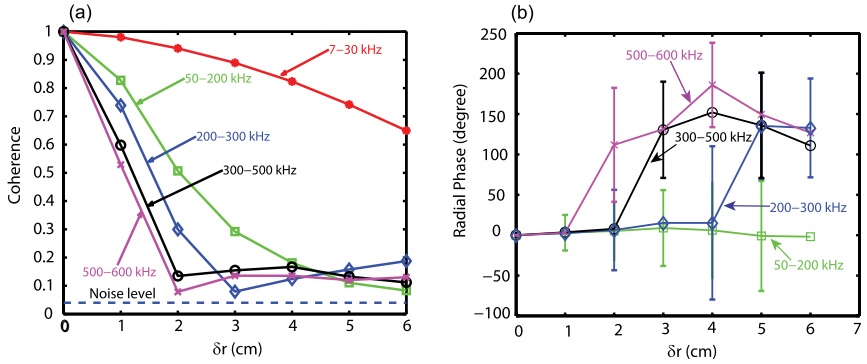


FIG. 5 (color online). (a) The radial coherence for $\tilde{B}_T$ in frequency ranges: 7–30 kHz, 50–200 kHz, 200–300 kHz, 300–500 kHz, and 500–600 kHz. (b) The radial phase of fluctuations in frequency ranges: 50–200 kHz, 200–300 kHz, 300–500 kHz, and 500–600 kHz with typical error bars. The error bars come from the statistical distribution of the radial phase: the lower the coherence, the larger the error bar.

it has both power-law and exponential scaling in the electron diamagnetic drift direction ($k_\perp < 0$). (Note that most of the fluctuation power at high $|k_\perp|$ propagates in the electron diamagnetic drift direction.) The exponential break in the cascade indicates onset of dissipation, often characterized by scale-dependent (or frequency-dependent) power laws, as could be fit to data like that in Fig. 1. Here we emphasize a comparison with recent scaling analysis for dissipation-range spectra as an improved model for this behavior. These model spectra have the generic form $S(k_\perp) \sim k_\perp^{-\alpha} \exp[-b(k_\perp/k_\eta)^\beta]$, where $\alpha = 5/3$ or $3/2$, $\beta = 4/3$ or $3/2$, and $b = 3/2$ or $4/3$, depending on the alignment of the flow and magnetic field fluctuations [9], and $k_\eta$ is the Kolmogorov wave number. A best fit of $S(k_\perp < 0)$ to this generic form gives $\alpha = 1.79$ with 95% confident bounds of (1.56, 2.02) and $\beta = 1.64$ with 95% confident bounds of (1.12, 2.16), which motivates our comparison with the model with $\alpha = 5/3$ since $\alpha = 3/2$ is marginally out of the 95% confident bounds of (1.56, 2.02). Thus we fit $S(k_\perp < 0)$ data to the model form of $S(k_\perp)/\mu_0\rho = E(k_\perp) = C_k \epsilon^{2/3} k_\perp^{-5/3} \exp(-3/2(k/k_\eta)^{4/3})$ [9], where $\rho$ is the plasma mass density $\sim 1 \times 10^{-8}$ kg $\cdot$ m$^{-3}$, $C_k$ is the Kolmogorov constant (of order of unity), $\epsilon$ is the energy dissipation rate, and $k_\eta = \epsilon^{1/4}/\eta^{3/4}$ ($\eta$ is the resistivity). The best fit, as shown in Fig. 4, yields $\epsilon = 2 \times 10^{12}$ m$^2 \cdot$ s$^{-3}$ (we assume that $C_k \approx 1$) and $k_\eta \approx 0.8$ cm$^{-1}$ which is about 4 times smaller than calculated $k_\eta = 3$ cm$^{-1}$ with the same $\epsilon$ but using classical resistivity of 5 m$^2 \cdot$ s$^{-1}$ calculated using local plasma parameters. This suggests that noncollisional dissipation of the turbulence may be important, a feature possibly related to the noncollisional ion heating that is also observed in MST plasmas [10–12].

In inhomogeneous plasmas, magnetic turbulence could be localized in the radial direction due to the equilibrium density gradient or magnetic shear. The radial structure of the turbulence was measured using a magnetic probe with 7 radially separated pickup loops to obtain the radial phase and coherence, shown in Fig. 5. Panel (a) shows the radial coherence of $\tilde{B}_T$ in five frequency bands: 7–30 kHz, 50–200 kHz, 200–300 kHz, 300–500 kHz, and 500–600 kHz. Since 7–30 kHz corresponds to global tearing mode frequencies, a large radial correlation length is expected and observed ($e$-folding length more than 10 cm). For higher frequency fluctuations the radial coherence drops rapidly relative to the reference point ($\delta r = 0$ cm), and the $e$-folding length is about 1.5–2.5 cm. This radial localization of the high frequency fluctuations corroborates the local resonant feature discussed above in connection with Fig. 2(b). The radial phase of the higher frequency fluctuations is shown in panel (b). If the fluctuations propagate in the radial direction, a continuous phase change for different frequencies is expected. This is not observed, rather the radial phase is either 0 or about $\pi$. For example, the radial phase in the 50–200 kHz band remains 0 for the entire 6 cm radial span. On the other hand, the radial phase in the 200–300 kHz band has a phase jump from 0 to about $\pi$ at $\delta r = 4$ cm. The other two frequency bands show similar behavior, with the phase jump location occurring at smaller radial separation as the frequency increases, indicating the $e$-folding length decreases for increasing frequency. This behavior reveals a radial standing wave structure for the fluctuations. Two electromagnetic modes, the collisional shear Alfvén mode [23] and microtearing mode [24], may have this type of radial structure, and are therefore good candidates to describe the short wavelength magnetic fluctuations. While it is unclear whether the observed standing wave structure could be a result of any inherent property of reversed field pinch plasmas, the bounded nature of laboratory plasmas certainly contributes. Furthermore, we expect the standing wave structure to exist in other laboratory plasmas since the existence of the two electromagnetic modes is not limited to reversed field pinch plasmas.

In summary, fully developed magnetic turbulence with strong anisotropy is observed in a reversed field pinch plasma. The anisotropy has $\Delta k_\perp \gg \Delta k_{||}$ with respect to

the background magnetic field, a feature that is consistent with Alfvénic turbulence, e.g., Ref. [19], and extends to fluctuations in the ion cyclotron frequency range. The fluctuation spectra exhibit features consistent with a nonlinear turbulent energy cascade driven by unstable tearing modes at the global scale. The scaling of the fluctuations has both power-law and exponential character consistent with inertial and dissipation processes [9,19], but the inferred dissipation of fluctuations propagating in the electron diamagnetic direction appears to be noncollisional in nature. The high frequency, smaller scale fluctuations exhibit a radial standing wave structure which is reminiscent of the linear structure for collisional shear Alfvén and microtearing modes [23,24].

The authors are grateful to the MST research team for their excellent help and support. This work is funded by DOE and NSF.

*Present address: Princeton Plasma Physics Laboratory, Princeton, NJ 08543.
yren@pppl.gov

[1] J. W. Belcher and L. D. Jr, J. Geophys. Res. **76**, 3534 (1971).
[2] C. C. Chaston *et al.*, Phys. Rev. Lett. **100**, 175003 (2008).
[3] S. C. Prager, Plasma Phys. Controlled Fusion **32**, 903 (1990).
[4] S. A. Balbus and J. F. Hawley, Rev. Mod. Phys. **70**, 1 (1998).
[5] G. Fiksel *et al.*, Phys. Rev. Lett. **103**, 145002 (2009).
[6] W. X. Ding *et al.*, Phys. Rev. Lett. **103**, 025001 (2009).
[7] W. H. Matthaeus, M. L. Goldstein, and D. A. Roberts, J. Geophys. Res. **95**, 20673 (1990).
[8] O. Alexandrova *et al.*, Phys. Rev. Lett. **103**, 165003 (2009).
[9] P. W. Terry and V. Tangri, Phys. Plasmas **16**, 082305 (2009).
[10] E. Scime *et al.*, Phys. Fluids B **4**, 4062 (1992).
[11] V. Tangri, P. W. Terry, and G. Fiksel, Phys. Plasmas **15**, 112501 (2008).
[12] R. M. Magee *et al.*, Phys. Rev. Lett. **107**, 065005 (2011).
[13] R. N. Dexter, D. W. Kerst, T. W. L. amd, S. C. Prager, and J. C. Sprott, Fusion Technol. **19**, 131 (1991).
[14] J. M. Beall, Y. C. Kim, and E. J. Powers, J. Appl. Phys. **53**, 3933 (1982).
[15] S. Hokin *et al.*, Phys. Fluids B **3**, 2241 (1991).
[16] H. Ji, A. F. Almagri, S. C. Prager, and J. S. Sarff, Phys. Rev. Lett. **73**, 668 (1994).
[17] S. Ortolani and D. D. Schnack, *Magnetohydrodynamics of Plasma Relaxation* (World Scientific, Singapore, 1993).
[18] D. Montegomery and L. Turner, Phys. Fluids **24**, 825 (1981).
[19] S. Sridhar and P. Goldreich, Astrophys. J. **432**, 612 (1994).
[20] W. H. Matthaeus, S. Ghosh, S. Oughton, and D. A. Roberts, J. Geophys. Res. **101**, 7619 (1996).
[21] G. I. Taylor, Proc. R. Soc. A **164**, 476 (1938).
[22] J. S. Sarff *et al.*, Phys. Plasmas **2**, 2440 (1995).
[23] J. F. Drake and R. G. Kleva, Phys. Fluids **24**, 1499 (1981).
[24] N. T. Gladd, J. F. Drake, C. L. Chang, and C. S. Liu, Phys. Fluids **23**, 1182 (1980).